

Developments in full seismic waveform tomography on continental scales

Andreas Fichtner¹, Paul Käufel², Brian L. N. Kennett³, Jeannot Trampert¹, Heiner Igel² & Hans-Peter Bunge²

¹ Department of Earth Sciences, Utrecht University, Utrecht, The Netherlands

² Department of Earth and Environmental Sciences, University of Munich, Munich, Germany

³ Research School of Earth Sciences, The Australian National University, Canberra, Australia

Introduction

Recent progress in computational seismology allows us today to simulate the propagation of seismic waves through 3D heterogeneous Earth models with unprecedented accuracy. These new capabilities can now be used to further our understanding of the Earth's structure and dynamics.

Full waveform tomography (FWT) is a tomographic technique that takes advantage of numerical solutions of the elastic wave equation. Numerically computed seismograms automatically contain the complete seismic wavefield, including all body and surface wave phases, as well as scattered waves generated by lateral variations of the model Earth properties. The amount of exploitable information is thus significantly larger than in tomographic methods that are based, for instance, on measurements of surface wave dispersion or the arrival times of specific seismic phases. The accuracy of the numerical solutions and the exploitation of complete waveform information result in tomographic images that are both more realistic and better resolved (TAPE et al. 2009, FICHTNER et al. 2009; 2010a, FICHTNER 2010).

Here we present applications of FWT to continental-scale problems. We pay special attention to the following issues: (1) the solution of the forward problem, (2) the quantification of waveform differences, (3) the iterative inversion based on adjoint techniques, and (4) the analysis of resolution with the help of probabilistic and deterministic approaches. The tomographic images provide new insight into the structure and dynamics of the upper mantle beneath Australia and Europe.

Solution of the forward problem

One of the principal advantages of FWT is the accurate solution of the elastic wave equation in laterally heterogeneous Earth models with the help of numerical methods. High accuracy is particularly important for surface waves that are mostly sensitive to strong material contrasts in the lithosphere. A precise solution ensures that the misfit between data and synthetics is primarily caused by imprecise source parameters and the differences between the mathematical model Earth and the real Earth.

Several methods have been developed for the solution of the 3D elastic wave equation, each being well suited for particular problems. These methods include, but are not limited to, finite-difference schemes (e.g. IGEL et al. 2002, BOHLEN 2002), their optimal operator variants (e.g. TAKEUCHI & GELLER 2000) and discontinuous Galerkin methods (e.g. DUMBSER & KÄSER 2006). For seismic wave propagation on continental and global scales, the spectral-element method (SEM) has proven to be a working compromise between accuracy and computational efficiency (e.g. FACCIOLI et al. 1997, KOMATITSCH & TROMP 2002). The SEM requires a comparatively small number of grid points per wavelength, and the free-surface boundary condition is automatically accounted for by solving the weak form of the equations of motion. The correct treatment of the free-surface condition ensures the accurate simulation of surface waves that make up more than 90 per cent of the waveforms in our data set.

We have implemented an SEM variant that operates in a spherical section where both viscoelastic dissipation and anisotropy can be modelled (FICHTNER & IGEL 2008). The artificial bounda-

ries of the spherical section are treated with the anisotropic perfectly matched layers technique (APML) proposed by TEIXEIRA & CHEW (1997) and ZHENG & HUANG (2002). To reduce the computational costs of the forward problem solution, we implemented a smooth long-wavelength equivalent model of the crust derived from crust 2.0 (BASSIN et al. 2000) that allows us to use a coarser grid spacing (FICHTNER & IGEL 2008). The crustal part of the model is also updated during the inversion, thus reducing the effect of potential inaccuracies in the initial crustal model.

Misfit quantification and minimisation

The resolution of tomographic images depends on the amount of data that enters the inversion process. To extract as much waveform information as possible while conforming to the restrictions imposed by the physics of the problem, we measure time-frequency phase misfits (FICHTNER et al. 2008). They quantify the phase differences between observed and synthetic waveforms at different times and for a continuous range of frequencies. The principal advantages of the time-frequency phase misfits are (1) a quasi-linear relation to 3D Earth structure, (2) applicability to all types of seismic waves, including interfering phases that are commonly observed at regional distances, and (3) independence from absolute amplitudes that are strongly influenced by shallow structures such as sedimentary basins.

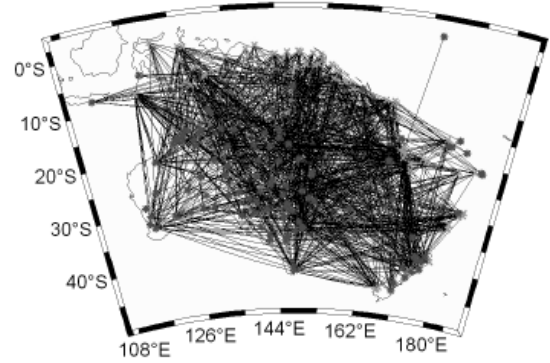


Fig. 1: Ray coverage used in the full waveform tomographic study.

To minimise the cumulative phase misfit of all stations, we implemented a pre-conditioned conjugate-gradient algorithm that updates the Earth model iteratively starting from a 3D initial model that represents the very long wavelength structure of the study region.

The gradient of the misfit functional can be computed most efficiently with the help of adjoint techniques (e.g. TARANTOLA 1988, FICHTNER et al. 2006): Following the simulation and storage of the forward wavefield, \mathbf{u} , for the current model, the misfit is evaluated. The misfit functional then determines the adjoint source, which is the right-hand side of the adjoint wave equation. Solving the adjoint wave equation with the help of the SEM gives the adjoint wavefield, \mathbf{u}^t . Finally, \mathbf{u} and \mathbf{u}^t are spatially correlated to yield the gradient of the misfit functional with respect to the Earth model parameters.

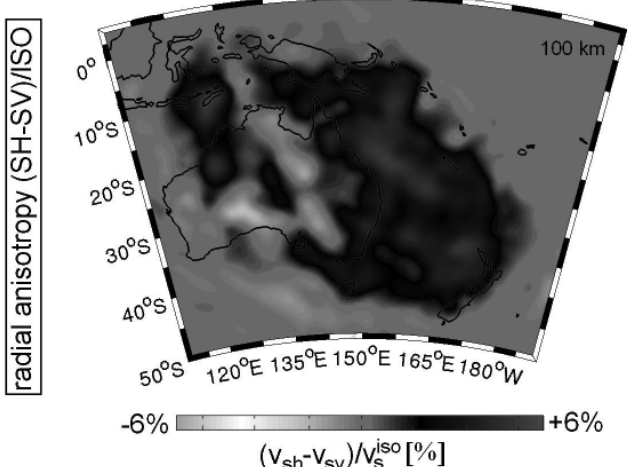
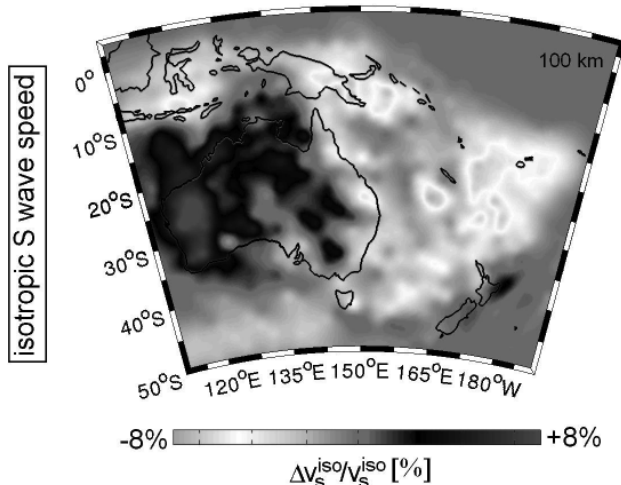


Fig. 2: Horizontal slices through the upper-mantle model AMSAN.19. **Left:** Isotropic S wave speed at 100 km depth. **Right:** Radial anisotropy at 100 km depth, expressed in terms of the relative difference between the SH and SV wave speeds.

FWT for upper-mantle structure in the Australasian region

We first applied our FWT method to the imaging of radially anisotropic upper-mantle structure in the Australasian region (FICHTNER et al. 2009). Our data set consists of 2137 three-component recordings from permanent stations operated by Geoscience Australia, IRIS and GEOSCOPE and from temporary networks operated by The Australian National University. We manually selected time windows where the observed waveforms show a clear correspondence to the synthetics. The resulting set of waveforms comprises fundamental- and higher-mode surface waves, long-period body waves and unidentified phases. The periods of the waveforms range between 30 s and 200 s, thus ensuring that struc-

ture to depths of around 350 km can be resolved. The ray coverage, shown in figure 1, is good throughout the eastern part of the continent and decreases towards the west.

After 19 iterations we obtained our preferred model, AMSAN.19, shown in figure 2. The iterative improvement of the tomographic model leads to the recovery of realistic absolute velocities that are necessary for the accurate prediction of seismic waveforms. The resolution of the tomographic images, estimated from a series of synthetic inversions, is around 3° laterally and 40 km vertically (FICHTNER et al. 2010a).

AMSAN.19 is able to predict complete three-component seismic waveforms in the period range from 30 s to 200 s with unprecedented

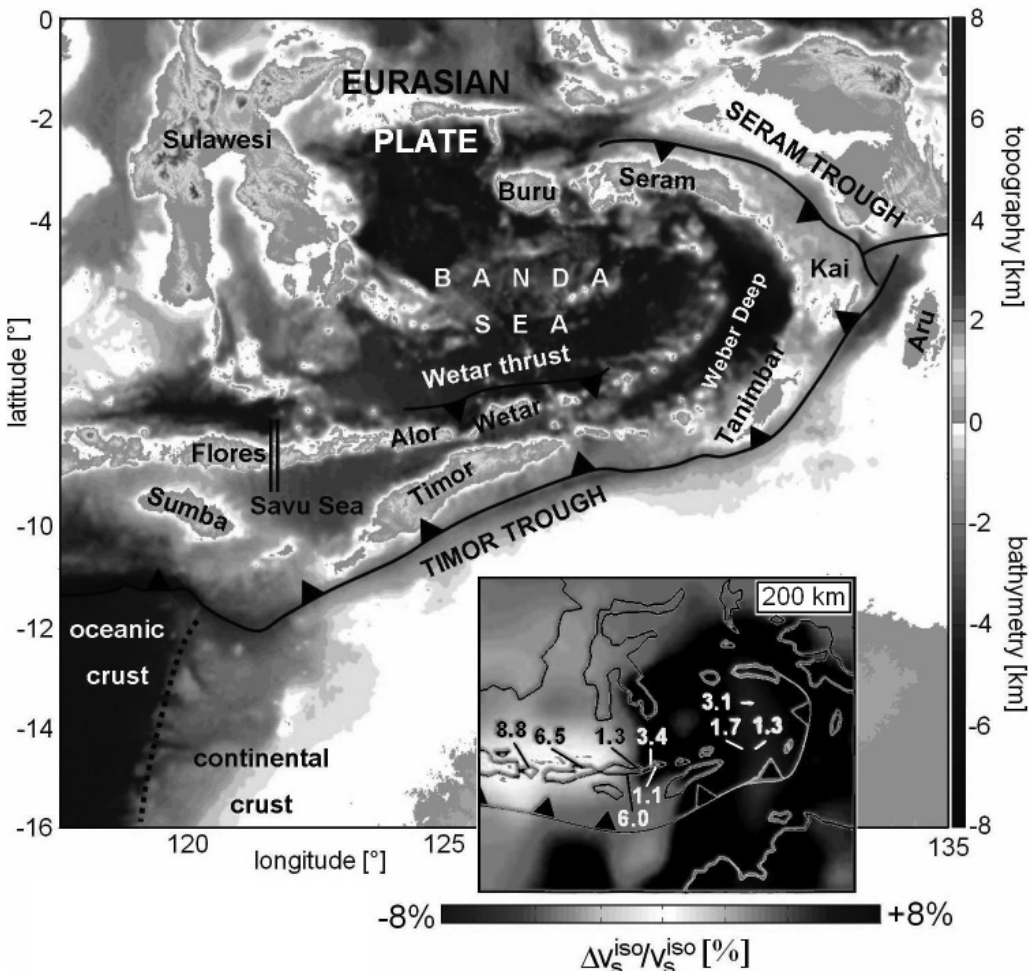


Fig. 3: Tectonic setting of the Banda Arc region with topographic data from ETOPO1 (AMANTE & EAKINS 2009) and trench locations after BIRD (2003). The double line across Flores marks the east–west transition from high $^{3}\text{He}/^{4}\text{He}$ ratios ($\approx 8\text{RA}$) to low $^{3}\text{He}/^{4}\text{He}$ ratios ($\approx 1\text{RA}$), respectively, where RA is the helium isotope ratio of air. The inlay shows the isotropic S wave speed variations from AMSAN.19 in the Banda Arc region at 200 km depth. Superimposed is a selection of He isotope ratios as measured by HILTON & CRAIG (1989) and HILTON et al. (1992).

accuracy (FICHTNER et al. 2010a). In a pilot study we found that the 3D tomographic model can be used to improve moment tensor solutions that are commonly inferred with the help of 1D Earth models (HINGEE et al. 2010). This opens the door towards more reliable tsunami warnings for the Australasian region.

One of the most remarkable features in the tomographic images can be found along the Banda Arc, near the triple junction of the Eurasian, Australian and Pacific plates (figure 3, FICHTNER et al. 2010b). There we observe a previously unrecognised coincidence of transitions in He, Pb, Sr and Nd isotope ratios (e.g. HILTON et al. 1992, VROON et al. 1993, ELBURG et al. 2005) in eastern Flores with the transition from lower wave speeds beneath the eastern Sunda Arc to higher wave speeds beneath the Banda Arc. This coincidence supports the direct transfer of compositional information from isotope measurements into the tomographic images. Low ${}^3\text{He}/{}^4\text{He}$ isotope ratios ($\approx 1.0\text{--}3.4\text{R}_A$, $\text{R}_A = {}^3\text{He}/{}^4\text{He}$ ratio of air) combined with He abundances (HILTON et al. 1992) and the isotope signatures of Pb, Sr and Nd (e.g. VROON et al. 1993, ELBURG et al. 2005) are consistent with the presence of conti-

nental crust at more than 150 km depth beneath the Banda Arc. This suggests the association of the high-velocity material with continental rather than oceanic lithosphere. The predominance of oceanic lithosphere, and thus of oceanic crust, would result in He isotope ratios around 6.0–8.0 R_A , as are typically found along circum-Pacific arcs and the Sunda Arc east of the He transition (POREDA & CRAIG 1989).

Probabilistic FWT based on tectonic regionalisation

The FWT described in the previous paragraph is deterministic in the sense that it results in one single Earth model that explains most of the observed waveforms. While being useful in the detection of smaller-scale features, the deterministic approach does not appraise the non-uniqueness that is inherent in any tomographic inversion. Chequerboard tests and the correlation of tomographic images with independent data (e.g. isotope signatures or well logs) are indicators of resolution, but a complete uncertainty and trade-off analysis requires a probabilistic approach (e.g. TARANTOLA 2005).

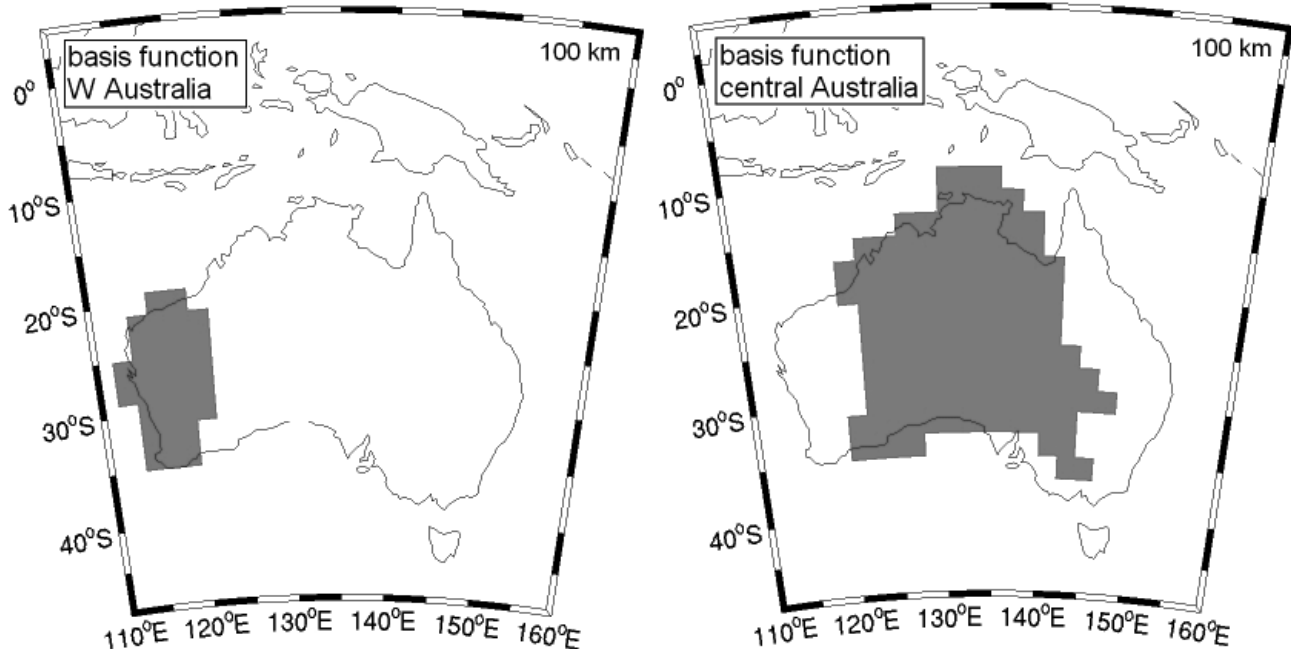


Fig. 4: Basis functions for the upper parts of the Archean lithosphere (left) and the Proterozoic lithosphere (right), plotted at 100 km depth. The outline of the basis functions is based on previous tomographic studies where the Precambrian units of the Australian lithosphere have been identified consistently (e.g. DEBAYLE & KENNEDY 2000, SIMONS et al. 2002, FISHWICK & READING 2008, FICHTNER et al. 2009)

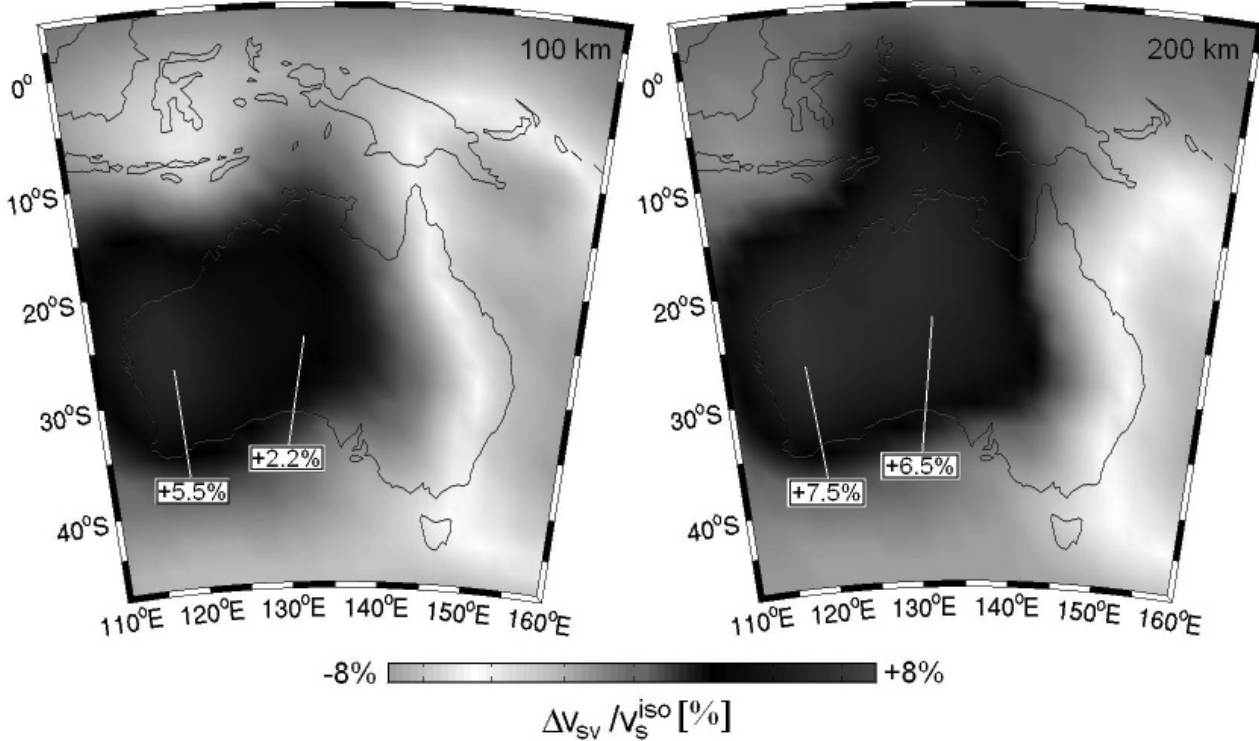


Fig. 5: S velocity distribution of a random Earth model (samples) plotted at 100 km and 200 km depth. The background model is PREM (DZIEWONSKI & ANDERSON 1981)

To limit the computational costs of a fully probabilistic inversion to a feasible level, we adopted a regionalised model parameterisation. For this we define the basis functions of the model space such that they coincide with (1) the upper (40–150 km depth) and lower (150–240 km depth) parts of the western Australian lithosphere that is predominantly Archean, and (2) the upper (40–150 km depth) and lower (150–240 km depth) parts of the mostly Proterozoic lithosphere in central Australia. The upper basis functions at 100 km depth are shown in figure 4.

The model parameters are density, ρ , the S velocity, v_s , and the P velocity, v_p . It follows that the parameter space is 12-dimensional (4 basis functions times 3 parameters). The structure defined by the linear combination of the basis functions is embedded within the tomographic model AMSAN.19 (figure 2). Smoothing is applied to prevent the generation of artifacts along the sharp boundaries of the basis functions. This regionalised parameterisation of the model space is intended to answer concrete geologic questions, concerning for instance, the reliability of the very high velocities beneath the Archean cratons in western Australia. It furthermore allows us to generate 3D random Earth models

efficiently by simply perturbing the 12 model parameters that define the elastic structure within the basis functions. Two examples of randomly generated Earth models are shown in figure 5.

With the help of the Neighbourhood Algorithm (SAMBRIDGE 1999) we sampled the parameter space by computing SEM synthetics for nearly 5000 random models. This led to an estimate of the posterior probability distribution (PPD) that reflects the resolution of and the trade-offs between model parameters.

The marginal PPDs in figure 6 confirm that the S velocity in the upper layer (40–150 km depth) is elevated relative to the radially symmetric Earth model PREM (DZIEWONSKI & ANDERSON 1981). The most likely S velocity perturbation within the Archean is around 0.35 km/s ($\approx 8\%$). As suggested already by FISHWICK & READING (2008) and FICHTNER et al. (2010a), the upper part of the Proterozoic lithosphere differs substantially from its Archean counterpart in western Australia. The S velocity is still elevated but unlikely to exceed 0.3 km/s. A detailed interpretation of the PPD in terms of the physics of wave propagation and the nature of the Australian lithosphere is work in progress.

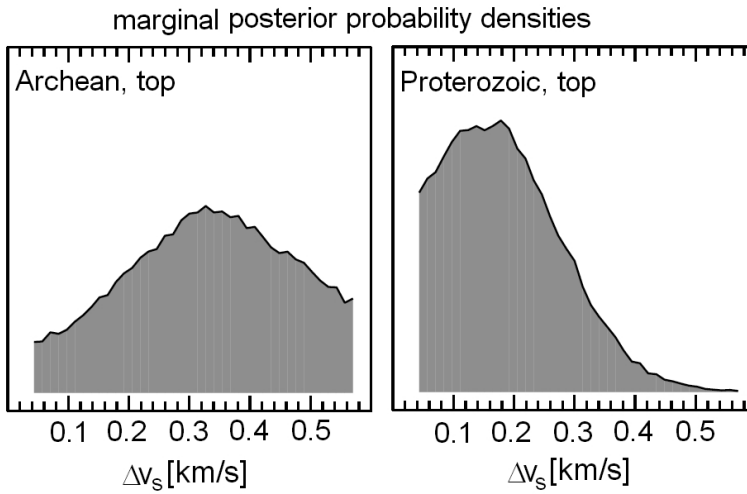


Fig. 6: Marginal posterior probability densities for the absolute S velocity perturbations relative to PREM (DZIEWONSKI & ANDERSON 1981) within the Archean (left) and the Proterozoic (right) at depths between 40 km and 150 km (top basis functions).

FWT for the European upper mantle: Towards the quantitative resolution and trade-off analysis in deterministic waveform tomography

Limited computational resources restrict the probabilistic approach to problems where the dimension of the parameter space is small, typically below 100. As part of our effort to develop methods for quantitative resolution analysis in large-scale deterministic FWT, we generalised the time-domain adjoint method such that it allows for the efficient calculation of second derivatives, which are the carriers of covariance information in the vicinity of the optimal model (FICHTNER 2010). Each row of the Hessian can be computed by correlating the forward wavefield with a primary and a secondary adjoint wavefield. Since the propagation of both adjoint fields is governed by the elastic wave equation, pre-existing codes do not need to be modified.

Moreover, formulas for the computation of Fréchet kernels can be reused for the computation of Hessian kernels, which are defined as the volumetric densities of the second derivatives. The Hessian kernels can be interpreted as resolution and trade-off (RETRO) kernels that provide information on where a specific 3D heterogeneity trades off with structure in other regions of the Earth model.

To illustrate the RETRO kernel concept we consider a long-period full waveform tomography for the European upper mantle that is summarised in figure 7. The data used in the inversion are three-component seismograms with a dominant period of 100 s, that provide a good coverage of central and northern Europe (figure 7, left). The inversion was based on the measurement of time- and frequency-dependent phase differences as described above (FICHTNER et al. 2008). As initial model we used the 3D mantle

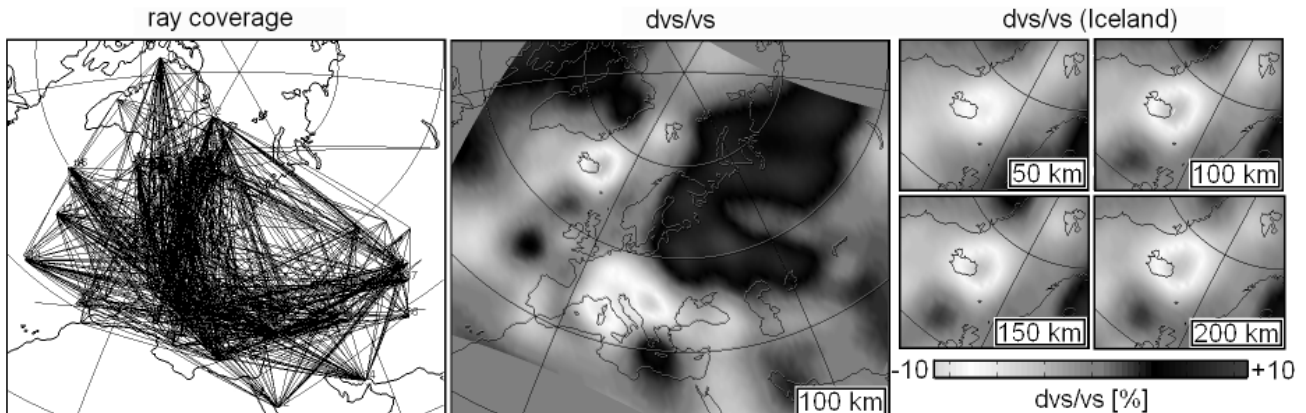


Fig. 7: Full waveform tomography for the European upper mantle. **Left:** Ray coverage. **Centre:** Relative v_s perturbations at 100 km depth. **Right:** Zoom on the Iceland hotspot at various depth levels. The background model is PREM (DZIEWONSKI & ANDERSON 1981).

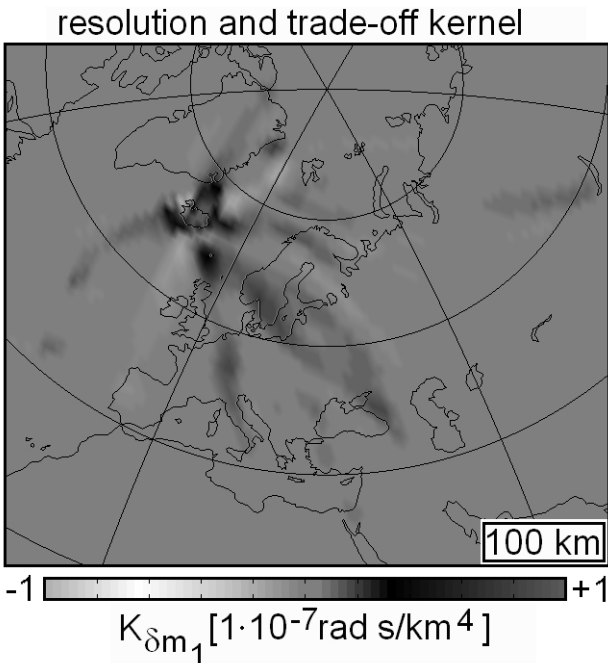


Fig. 8: Resolution and trade-off (RETRO) kernel at 100 km depth. The kernel corresponds to an S velocity perturbation that extends from 80 km to 130 km depth directly beneath Iceland. The non-zero contributions to the RETRO kernel outline those regions of the European upper mantle that affect our image of the Iceland plume at 80-130 km depth.

structure from S20RTS (RITSEMA et al. 1999) combined with the crustal model by MEIER et al. (2007a, b). After 3 conjugate-gradient iterations we obtained the tomographic images shown in the centre and left panels of figure 7. One of the most prominent features is the low-velocity region beneath Iceland, that is commonly attributed to the high temperatures of a mantle plume associated with the Mid-Atlantic ridge.

To quantify the extent to which the plume structure is independently constrained, we consider an S velocity perturbation within a test volume that extends from 80 km to 130 km depth beneath Iceland. Using the extended adjoint method, we compute the column of the Hessian that corresponds to the test volume, i.e. the RETRO kernel for the plume structure between 80 km and 130 km depth. The result is shown in figure 8. The RETRO kernel is a superposition of mostly positive arms that extend from the test volume towards several source and receiver positions. The non-zero contributions of the RETRO kernel are those regions where the v_s structure of

the plume trades off with the v_s structure in other parts of the European upper mantle. It follows that the low S velocities seen between 80 km and 130 km depth beneath Iceland can not be constrained independently. Strong contributions to our image of the plume structure come from north-eastern Europe and the upper mantle surrounding Iceland.

Conclusions and Outlook

In this paper we reported on recent developments in continental-scale FWT based on the combination of spectral-element simulations of seismic wave propagation, the adjoint method and the measurement of time-frequency misfits. The purely numerical solutions of the seismic wave equation are accurate for realistically heterogeneous Earth models, and they allow us to exploit information from all types of seismic waveforms, including body waves, surface waves and oscillations that can not be classified in terms of standard seismological phases.

We have shown that 3D FWT for realistic problems is indeed feasible. It yields highly resolved tomographic images and an excellent fit to seismic waveforms including both body and surface waves. The joint interpretation of the tomographic images for the Australasian region and isotope signatures along the Banda Arc provides new insight into the subduction of Precambrian continental lithosphere. Promising approaches towards uncertainty quantification in FWT include the probabilistic inversion based on tectonic regionalisations and the RETRO kernel concept.

While FWT is already a powerful tool, further improvements are necessary in order to advance our understanding of 3D Earth structure. Future research will address (1) the simultaneous inversion for crust and mantle structure including crustal discontinuities, (2) multi-parameter inversions with a strong focus on 3D density and attenuation structure, (3) multi-scale FWT that combines local- to global-scale data sets, and (4) the quantitative analysis of resolution that goes beyond synthetic inversions and the subjective visual inspection of the results.

References

- AMANTE, C. & EAKINS, B. W. (2009): ETOPO1 1 arc-minute global relief model: Procedures, data sources and Analysis. – NOAA Technical Memorandum NESDIS NGDC-24.
- BASSIN, C., LASKE, G. & MASTERS, G. (2000): The current limits of resolution for surface wave tomography in North America. – EOS Transactions **81**: F897.
- BIRD, P. (2003): An updated digital model of plate boundaries. – Geochemistry Geophysics Geosystems **4**, doi: 10.1029/2001GC000252.
- BOHLEN, T. (2002): Parallel 3D viscoelastic finite difference modelling. – Computers & Geosciences **28**: 887-899.
- DEBAYLE, E. & KENNEDY, B. L. N. (2000): The Australian continental upper mantle: Structure and deformation inferred from surface waves. – Journal of Geophysical Research **105**: 25423-25450.
- DUMBSER, M. & KÄSER, M. (2006): An arbitrary high-order discontinuous Galerkin method for elastic waves on unstructured meshes - II. The three-dimensional isotropic case. – Geophysical Journal International **167**: 319-336.
- DZIEWONSKI, A. M. & ANDERSON, D. L. (1981): Preliminary reference Earth model. – Physics of the Earth and Planetary Interiors **25**: 297-356.
- ELBURG, M. A., FODEN, J. D., VAN BERGEN, M. J. & ZULKARNAIN, I. (2005): Australia and Indonesia in collision: geochemical sources of magmatism. – Journal of Volcanology and Geothermal Research **140**: 25-47.
- FACCIOLI, E., MAGGIO, F., PAOLUCCI, R. & QUARTERONI, A. (1997): 2D and 3D elastic wave propagation by a pseudo-spectral domain decomposition method. – Journal of Seismology **1**: 237-251.
- FICHTNER, A., BUNGE, H.-P. & IGEL, H. (2006): The adjoint method in seismology - I. Theory. – Physics of the Earth and Planetary Interiors **157**: 86-104.
- FICHTNER, A. & IGEL, H. (2008): Efficient numerical surface wave propagation through the optimization of discrete crustal models - a technique based on non-linear dispersion curve matching (DCM). – Geophysical Journal International **173**: 519-533.
- FICHTNER, A., KENNEDY, B. L. N., IGEL, H. & BUNGE, H.-P. (2008): Theoretical background for continental- and global-scale full-waveform inversion in the time-frequency domain. – Geophysical Journal International **175**: 665-685.
- FICHTNER, A., KENNEDY, B. L. N., IGEL, H. & BUNGE, H.-P. (2009): Full seismic waveform tomography for upper-mantle structure in the Australasian region using adjoint methods. – Geophysical Journal International **179**: 1703-1725.
- FICHTNER, A. (2010): Full seismic waveform modelling and inversion. – Heidelberg (Springer).
- FICHTNER, A., KENNEDY, B. L. N., IGEL, H. & BUNGE, H.-P. (2010a): Full waveform tomography for radially anisotropic structure: New insights into present and past states of the Australasian upper mantle. – Earth and Planetary Science Letters **290**: 270-280.
- FICHTNER, A., DE WIT, M. & VAN BERGEN, M. (2010b): Subduction of continental lithosphere in the Banda Sea region: Combining evidence from full waveform tomography and isotope ratios. – Earth and Planetary Science Letters **297**: 405-412.
- FISHWICK, S. & READING, A. M. (2008): Anomalous lithosphere beneath the Proterozoic of western and central Australia: A record of continental collision and intra-plate deformation? – Precambrian Research **166**: 111-121.

- HILTON, D. R. & CRAIG, H. (1989): A helium isotope transect along the Indonesian archipelago. – *Nature* **342**: 906-908.
- HILTON, D. R., HOOGEWERFF, J. A., VAN BERGEN, M. J. & HAMMERSCHMIDT, K. (1992): Mapping magma sources in the east Sunda-Banda arc, Indonesia: Constraints from helium isotopes. – *Geochimica et Cosmochimica Acta* **56**: 851-859.
- HINGEE, M., TKALCIC, H., FICHTNER, A. & SAMBRIDGE, M. (2010): Moment tensor inversion using a 3-D structural model: Applications for the Australian region. – *Geophysical Journal International*, under review.
- IGEL, H., NISSEN-MEYER, T. & JAHNKE, G. (2002): Wave propagation in 3D spherical sections. Effects of subduction zones. – *Physics of the Earth and Planetary Interiors* **132**: 219-234.
- KOMATITSCH, D. & TROMP, J. (2002): Spectral-element simulations of global seismic wave propagation - I. Validation. – *Geophysical Journal International* **149**: 390-412.
- MEIER, U., CURTIS, A. & TRAMPERT, J. (2007A): Global crustal thickness from neural network inversion of surface wave data. – *Geophysical Journal International*, **169**: 706-722.
- MEIER, U., CURTIS, A. & TRAMPERT, J. (2007B): Fully nonlinear inversion of fundamental mode surface waves for a global crustal model. – *Geophysical Research Letters* **34**: doi: 10.1029/2007GL030989.
- POREDA, R. & CRAIG, H. (1989): Helium isotope ratios in circum-Pacific volcanic arcs. – *Nature* **338**: 473-478.
- RITSEMA, J., VAN HEIJST, H. J. & WOODHOUSE, J. H. (1999): Complex shear velocity structure imaged beneath Africa and Iceland. – *Science* **286**: 1925-1928.
- SAMBRIDGE, M. (1999): Geophysical inversion with a neighbourhood algorithm – I. Searching a parameter space. – *Geophysical Journal International* **138**: 479-494.
- SIMONS, F. J., VAN DER HILST, R. D., MONTAGNER, J.-P. & ZIELHUIS, A. (2002): Multimode Rayleigh wave inversion for heterogeneity and azimuthal anisotropy of the Australian upper mantle. – *Geophysical Journal International* **151**: 738-754.
- TAKEUCHI, N. & GELLER, R. J. (2000): Optimally accurate second-order time-domain finite difference scheme for computing synthetic seismograms in 2-D and 3-D media. – *Physics of the Earth and Planetary Interiors* **119**: 99-131.
- TAPE, C., LIU, Q. Y., MAGGI, A. & TROMP, J. (2009): Adjoint tomography of the southern California crust. – *Science* **325**: 988-992.
- TARANTOLA, A. (1988): Theoretical background for the inversion of seismic waveforms, including elasticity and attenuation. – *Pure and Applied Geophysics* **128**: 365-399.
- TARANTOLA, A. (2005): Inverse problem theory and methods for model parameter estimation, 2nd edition. – Society for Industrial and Applied Mathematics, Philadelphia.
- TEIXEIRA, F. L. & CHEW, W. C. (1997): Systematic derivation of anisotropic pml absorbing media in cylindrical and spherical coordinates. – *IEEE Microwave and Guided Wave Letters* **7**: 371-373.
- VROON, P. Z., VAN BERGEN, M. J., WHITE, W. M. & VAREKAMP, J. C. (1993): Sr-Nd-Pb isotope systematics of the Banda arc, Indonesia: Combined subduction and assimilation of continental material. – *Journal of Geophysical Research* **98**: 22349-22366.
- ZHENG, Y. & HUANG, X. (2002): Anisotropic perfectly matched layers for elastic waves in cartesian and curvilinear coordinates. – MIT Earth Resources Laboratory, Consortium Report.